

<Original>

## Fast Neutron Dosimetry in Criticality Accidents

Seung Gy Ro and Chong Chul Yook\*

*Korea Atomic Energy Research Institute, Seoul, Korea*

*\*Dept. of Nuclear Engineering, Hanyang University, Seoul, Korea*

(Received February 11, 1976)

### —Abstract—

A suggestion has been made for neutron dosimetric techniques using activation and threshold detectors in criticality accidents. Neutron dosimetric parameters, namely, the fission spectrum-averaged cross-sections of some threshold reactions and fluence-to-dose conversion factors have been calculated by the use of an electronic computer.

It appears that detectors having comparatively high threshold energy give more fine information on spectral deformation in criticality accidents, while detectors with low threshold energy are of usefulness for measuring fast neutron fluence regardless of fissioning types. Unexpectedly it is found that the fission spectrum-averaged cross sections of the  $^{32}\text{S}(n, p)^{32}\text{P}$  reaction is not sensitive to analytical forms of fission neutron spectrum: the modified Cranberg and Maxwellian forms. In addition, the fluence-to-dose conversion factors seem to be insensitive to both spectral functions and fissioning types.

### 1. Introduction

Threshold activation methods are commonly used to determine fast neutron dose in criticality accidents.<sup>1-3)</sup> Although other techniques can provide much more detailed data, these methods remain most attractive for neutron dosimetry because of the small physical size of the detectors and their gamma-ray insensitivity. The problem, however, is to make reliable interpretation of the experimental data. Its reliability is depending on an accurate information as much as is obtainable on the neutron spectrum.

Various interpretation methods<sup>4-6)</sup> have

been proposed to derive the neutron spectrum from the detector responses. Among them, the spectral index method seems most practicable to adopt for neutron dosimetry in criticality accidents. This method was originally suggested by Grundl and Usner,<sup>6)</sup> and was successful to account for the fact that the spectrum is characterized by fissioning types. Its particular feature is to describe the physical meaning of fission. No longer this method is, however, applicable in usual cases of criticality accidents where fission neutrons are not completely free from contamination due to scattered or slowing-down neutrons.

It is the purpose of this study to propose a dosimetric technique for measuring fast

neutron dose with some activation and threshold detectors in such a case that the fission neutron spectrum is overlapped by the slowing-down spectrum. Neutron dosimetric parameters, that is, fission spectrum-averaged cross-sections and fluence-to-dose conversion factors were calculated with the help of an electronic computer.

## 2. Spectral Model

The neutrons produced in the fission process undergo collisions with their surrounding materials. There exists therefore, in critical assemblies, a neutron spectrum covering an extensive range of energies. The whole neutron spectrum in this study is, for convenience, divided into three energy regions: the thermal region consisting of neutrons in thermal equilibrium with moderator, the fast or fission region in which the neutrons from fission are emitted, and the intermediate energy or slowing-down region. It should be noted that this division is arbitrary and the neutron spectrum is a continuous function of energy with no clearly defined boundaries.

An assumption is made on the spectral model in the specified region: 1) in the thermal region the spectrum has the pure Maxwellian distribution with neutron velocities corresponding to a temperature of 20 .4°C, 2) the spectrum holds an inverse-energy function in the slowing-down region, i.e., 0.12eV to fission neutron energy, and 3) the spectral distribution of fast neutrons is characterized by uncollided fission neutrons.

The lower limit of 0.12eV in the slowing-down region was taken on the basis of Westcott convention,<sup>7)</sup> while the upper limit

chosen was based on the concept that the slowing-down neutrons have fast neutrons as their source. In the region of fission neutron energies the slowing-down spectrum may be weighted by the fraction of neutrons originating in the fission spectrum greater than certain energy  $E$ . This weighting is based on the fact that number of neutrons slowing down past a particular energy depends upon the number of neutrons originating at all energies above the one in question. The mathematical expression for the slowing-down spectrum may be thus written by

$$\phi_i(E) = \frac{\theta}{E} \int_E^{\infty} \tilde{N}(E) dE \quad (1)$$

where  $\phi_i(E)$  is the slowing-down spectrum,  $N(E)$  the normalized fission neutron spectrum, and  $E$  the neutron energy in MeV. Hereinafter,  $F(E)$  refers to the integral term in the right side of Eq. (1).  $\theta$  is the flux density of intermediate energy neutrons per  $\ln E$ , and is given by the well-known equation

$$\theta = \frac{\phi_{th} \sigma_0 g}{[R_{cd} - 1] \int_{E_{cd}}^{\infty} \sigma_{ac}(E) \frac{1}{E} dE} \quad (2)$$

Here  $\sigma_0$ : the activation cross-section for 2200m/sec neutron

$\sigma_{ac}(E)$ : the differential activation cross-section

$g$ : Westcott factor relating to nuclear temperature<sup>7)</sup>

$R_{cd}$ : Cd-ratio

$\phi_{th}$ : the thermal neutron flux density.

Integral term in denominator of Eq. (2) is often called by resonance integral, and its lower limit of integration  $E_{cd}$  is usually given by 0.5eV when 1mm thick Cd is employed. This

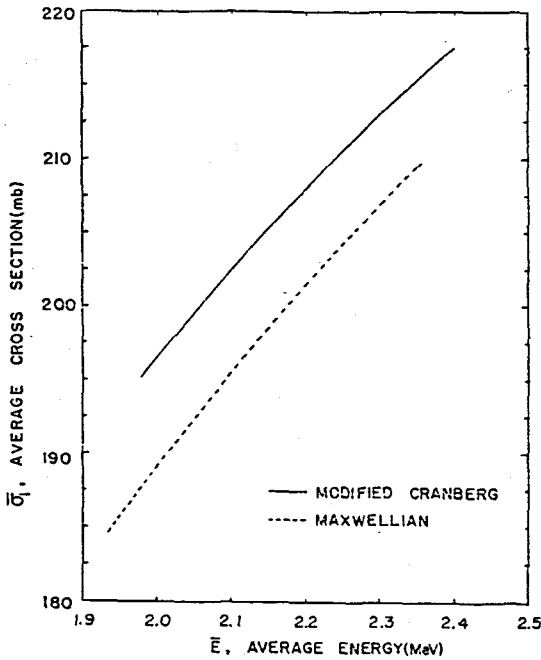


Fig. 1. Average cross-sections of  $^{115}\text{In}(n, n')^{115m}\text{In}$  reaction as a function of average fission neutron energies

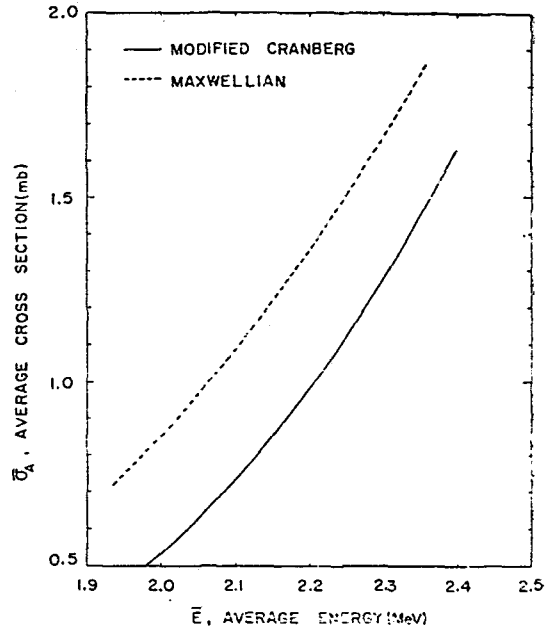


Fig. 3. Average cross-sections of  $^{27}\text{Al}(n, \alpha)^{24}\text{Na}$  reaction as a function of average fission neutron energies

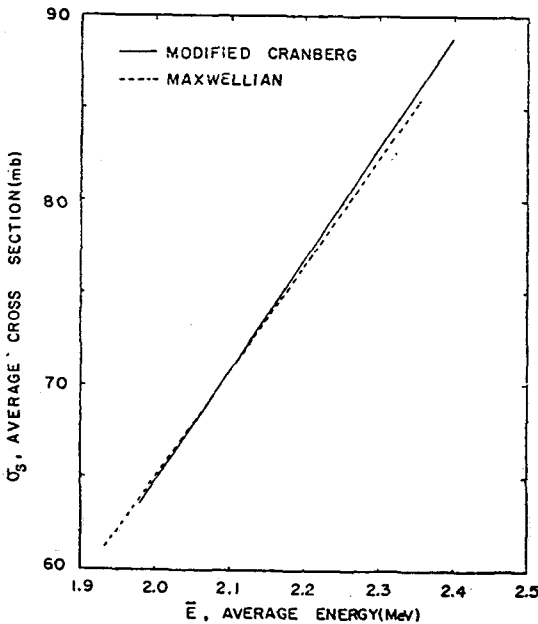


Fig. 2. Average cross-sections of  $^{32}\text{S}(n, p)^{32}\text{P}$  reaction as a function of average fission neutron energies

cut-off energy is competing with 0.12eV as aforementioned for the lower limit of the slowing-down spectrum. It should be added, however, that a contribution by neutrons in between is small enough to be neglected when there is no prominent resonance peak in the energy range of 0.12 to 0.5eV.

The normalized fission neutron spectrum is expressed by two representative formulae,

<sup>8, 9)</sup>  $N(E)$ , namely

$$N_c(E) = \frac{0.655}{(0.667E_c - 0.493)^{1/2}} \exp \left[ \frac{-0.74 + E}{(0.667E_c - 0.493)} \right] \text{sinh} \left( \frac{1.722E^{1/2}}{(0.667E_c - 0.493)} \right) \quad (3)$$

$$N_m(E) = \frac{0.463}{E_m} \left( \frac{E}{E_m} \right)^{1/2} \exp(-E/E_m) \quad (4)$$

where subscripts  $c$  and  $m$  stand for the modified Cranberg and Maxwellian forms, respectively.  $E$  is the neutron energy in

Table 1. Average cross-sections of some threshold reactions for neutron spectra from  $^{235}\text{U}+n$  (thermal) and  $+n(20\text{MeV})$  fissions

Fission type	Average cross-sections(mb)					
	Modified Cranberg form			Maxwellian form		
	$^{115}\text{In}(n, n')$	$^{32}\text{S}(n, p)$	$^{27}\text{Al}(n, \alpha)$	$^{115}\text{In}(n, n')$	$^{32}\text{S}(n, p)$	$^{27}\text{Al}(n, \alpha)$
$n$ (thermal) fission	195.14	63.47	0.50	184.62	61.19	0.72
$n$ (20MeV) fission	217.63	88.75	1.63	209.69	85.27	1.85
$\bar{\sigma}$ (for 20MeV fission)	1.12	1.40	3.21	1.14	1.39	2.57
$\bar{\sigma}$ (for thermal fission)						

MeV and  $\bar{E}$  the average fission neutron energy (throughout this work this terminology will be denoted by the average energy) that may describe the fissioning types in criticality accidents. A detailed description is made in the papers of Terrell<sup>8)</sup> and Ro et al.<sup>9)</sup>

### 3. Method

An interpretation of fast or fission neutron spectrum is made from the activation data of  $^{197}\text{Au}(n, \gamma)$ ,  $^{197}\text{Au}(n, \gamma)+\text{Cd}$ ,  $^{115}\text{In}(n, n')$ ,  $^{32}\text{S}(n, p)$ , and  $^{27}\text{Al}(n, \alpha)$  reactions.  $^{197}\text{Au}$  and  $^{197}\text{Au}+\text{Cd}$  were employed for measuring thermal and intermediate energy neutrons while the rest of three as threshold detectors were chosen for measurement of fast neutrons.

Obviously threshold detector is activated by both fast and intermediate energy neutrons when it is placed in critical assemblies. The apparent activity or response,  $R_s$ , to be induced in a threshold detector can be defined by

$$R_s = \phi_F \int_0^{\infty} \sigma(E) N(E) dE + \theta \int_0^{\infty} \bar{F}(E) \frac{\sigma(E)}{E} dE \quad (5)$$

in which  $\phi_F$  is the fast neutron flux density and  $\sigma(E)$  the excitation function of threshold reaction. The first and second terms of

righthand side in Eq. (5) represent a contribution by uncollided fission and intermediate energy neutrons, respectively.  $F(E)$  is clearly dependent on the fission neutron spectrum, but as a preliminary trial in this study is based on the thermal-induced  $^{235}\text{U}$  fission neutron spectrum.

The fast neutron spectrum is obtained by relating the spectral index determined by experiment to that of theoretical basis. The spectral index,  $S_{12}$ , is given by the ratio of responses indicated in two different detectors 1 and 2, viz:

$$S_{12E} \equiv \frac{R_{1r}}{R_{2r}} = \frac{R_{1r} - \theta \int_0^{\infty} \bar{F}(E) \frac{\sigma_1(E)}{E} dE}{R_{2r} - \theta \int_0^{\infty} \bar{F}(E) \frac{\sigma_2(E)}{E} dE} \quad (6a)$$

$$S_{12r} \equiv \frac{\bar{\sigma}_1}{\bar{\sigma}_2} = \frac{\int_0^{\infty} \sigma_1(E) N(E) dE}{\int_0^{\infty} \sigma_2(E) N(E) dE} \quad (6b)$$

Here  $\bar{\sigma}$  is the fission spectrum-averaged cross-section (hereinafter this terminology will be represented by average cross-sections), and subscript  $r$  in response  $R$  refers to the induced activity by fission neutrons while suffices  $E$  and  $T$  mean the spectral indices determined by experiment and theoretical basis, respectively. When the spectrum is determined, hencefrom fast neutron flux

**Table 2.** Comparison of average cross-sections ratio obtained by different spectral functions of fission neutrons

Fission type	Average cross-section ratio		
	$\bar{\sigma}_{TC}/\bar{\sigma}_{IM}$	$\bar{\sigma}_{SC}/\bar{\sigma}_{SM}$	$\bar{\sigma}_{AC}/\bar{\sigma}_{AM}$
$n$ (thermal) fission	1.057	1.037	0.694
$n$ (20MeV) fission	1.038	1.041	0.881
$\bar{\sigma}$ (for 20MeV fission)	0.982	1.004	1.270
$\bar{\sigma}$ (for thermal fission)			

**Table 3.** Computed kerma and maximum dose conversion factor per unit fluence for neutron spectra from  $^{235}\text{U}+n$ (thermal) and  $+n$ (20MeV) fissions

Fission type	Conversion factor			
	Modified Cranberg		Maxwellian	
	Kerma (rads/(n/cm <sup>2</sup> ))	Max. dose (rads/(n/cm <sup>2</sup> ))	Kerma (rads/(n/cm <sup>2</sup> ))	Max. dose (rads/(n/cm <sup>2</sup> ))
$n$ (thermal) fission	$2.83 \times 10^{-9}$	$3.61 \times 10^{-9}$	$2.83 \times 10^{-9}$	$3.61 \times 10^{-9}$
$n$ (20MeV) fission	$3.31 \times 10^{-9}$	$4.22 \times 10^{-9}$	$3.33 \times 10^{-9}$	$4.25 \times 10^{-9}$
$\bar{d}$ (for 20MeV fission)	1.17	1.17	1.18	1.18
$\bar{d}$ (for thermal fission)				

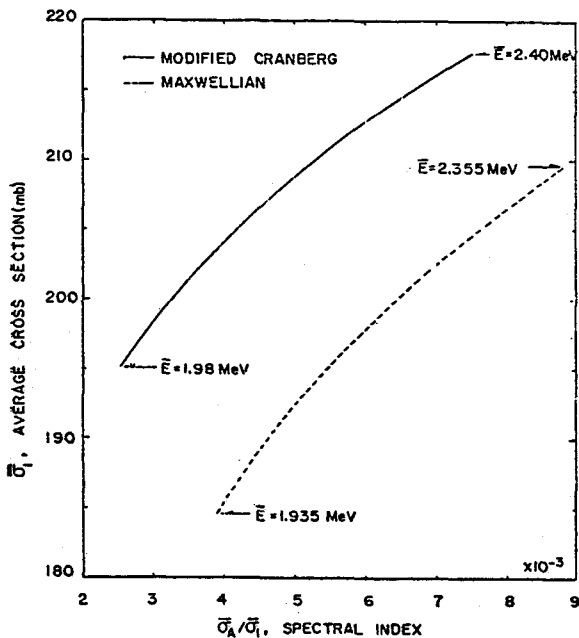


**Fig. 4.** Average cross-sections of  $^{115}\text{In}(n, n')$   $^{115}\text{In}$  reaction as a function of spectral index ( $\bar{\sigma}_A$ -to- $\bar{\sigma}_1$  ratio)

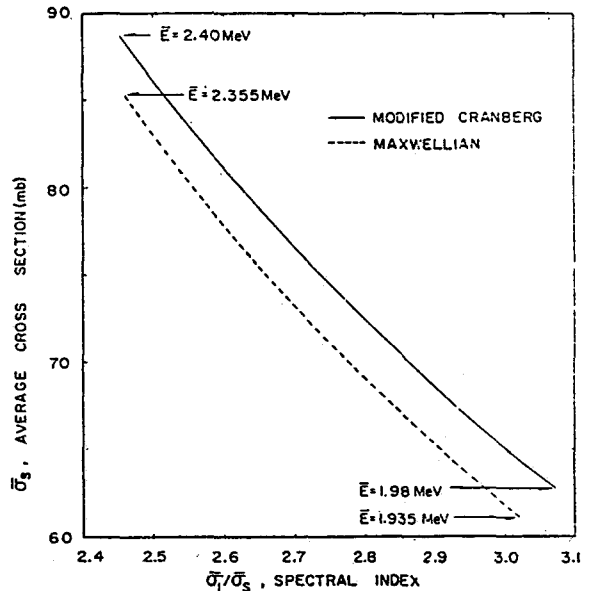


**Fig. 5.** Average cross-sections of  $^{32}\text{S}(n, p)^{32}\text{P}$  reaction as a function of spectral index ( $\bar{\sigma}_T$ -to- $\bar{\sigma}_3$  ratio)

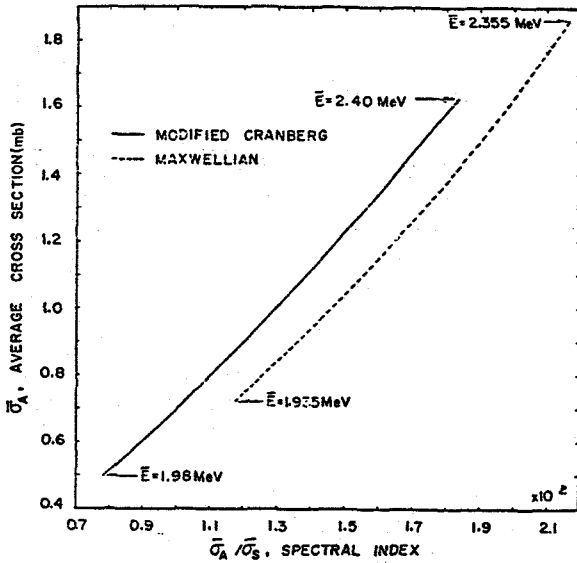


Fig. 6. Average cross-sections of  $^{27}\text{Al}(n, \alpha) ^{24}\text{Na}$  reaction as a function of spectral index ( $\bar{\sigma}_A$ -to- $\bar{\sigma}_S$  ratio)

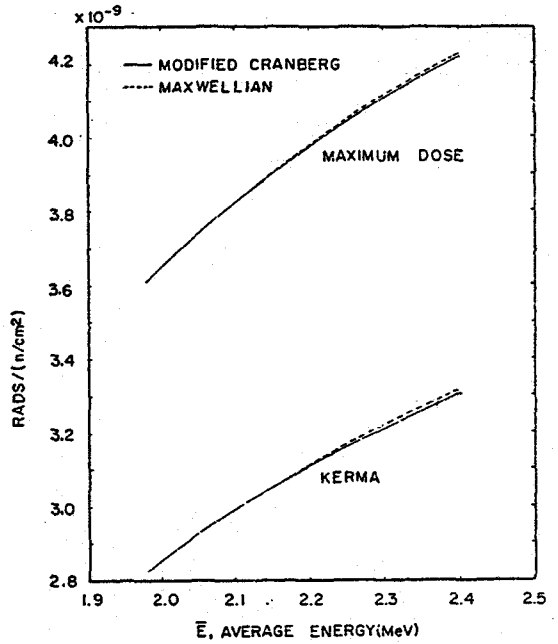


Fig. 7. Neutron fluence-to-dose conversion factor as a function of average fission neutron energies

density,  $\phi_F$ , is easily calculated from the activity induced in a single threshold detector,

$$\phi_F = \left( R_s - \theta \int_0^{\infty} F(E) \frac{\sigma(E)}{E} dE \right) / \int_0^{\infty} \bar{\sigma}(E) N(E) dE \quad (7)$$

and correspondingly neutron doses in terms of kerma and maximum dose,  $D$ , are computed by the equation.

$$D = \phi_F \int_0^{\infty} \bar{d}(E) N(E) dE \quad (8)$$

where  $d(E)$  is the differential dose.

#### 4. Calculation of Dosimetrical Parameters

The average cross-section,  $\bar{\sigma}$  is obtained by weighting the excitation function to the fission neutron spectrum [Eqs. (3) and (4)]. The excitation function of differential cross-sections for the  $^{115}\text{In}(n, n')$ ,  $^{32}\text{S}(n, p)$ , and

$^{27}\text{Al}(n, \alpha)$  reactions were taken from several published articles.<sup>10-15</sup> A numerical calculation of  $\bar{\sigma}$  was performed with varying average energy ( $\bar{E}$ ) in Eqs. (3) and (4) up to 20MeV of neutron energy by an electronic computer CYBER-73. Although the spectral function extends theoretically to infinite energy, only a small portion of contribution due to neutrons above 20MeV is expected so as to be disregarded. The average energy  $\bar{E}$ -values were varied from that corresponding to thermal-induced fission [1.98MeV in Eqs. (3) and 1.935MeV in Eq. (4)] up to that of 20MeV fission [2.40MeV in Eq. (3) and 2.335 MeV in Eq. (4)].<sup>16</sup>

The fluence-to-dose conversion factor,  $\bar{d}$ , is defined by

$$\bar{d} = \int_0^{\infty} \bar{d}(E) N(E) dE / \int_0^{\infty} N(E) dE \quad (9)$$

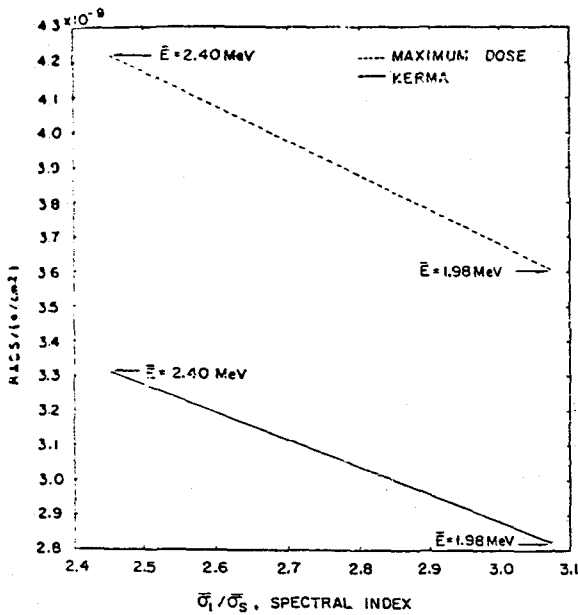


Fig. 8. Computed kerma and maximum dose conversion factor for modified Cranberg form as a function of spectral index ( $\bar{\sigma}_I$ -to- $\bar{\sigma}_S$  ratio)

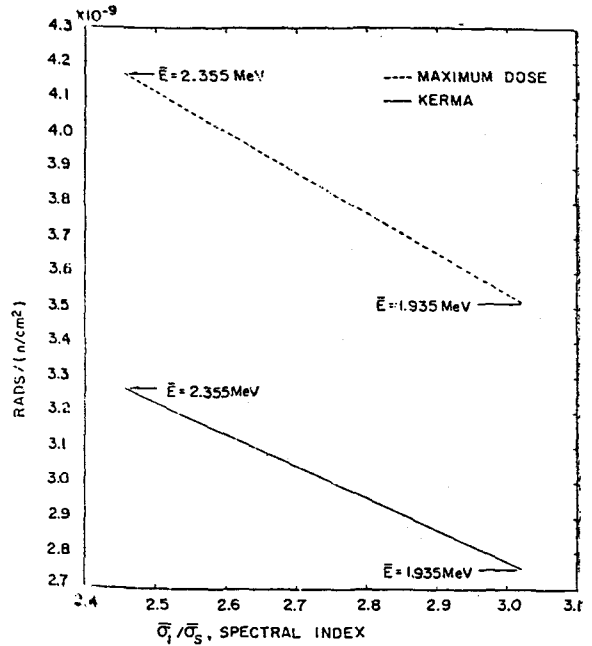


Fig. 9. Computed kerma and Maximum dose conversion factor for Maxwellian form as a function of spectral index ( $\bar{\sigma}_I$ -to- $\bar{\sigma}_S$  ratio)

in which  $d(E)$  is the differential dose in terms of kerma and maximum dose, and was mainly extracted from reports.<sup>17, 18)</sup>

The autogamma dose from the  ${}^1\text{H}(n, \gamma){}^2\text{D}$  reaction in the human body was exempted from the calculation of  $\bar{d}$  based on the maximum dose, since it can be readily obtained by the conventional film dosimetry.

## 5. Results and Discussion

In Figs. 1-3 shown is a relationship of average cross-sections ( $\bar{\sigma}$ ) vs average fission neutron energy ( $\bar{E}$ ) for the  ${}^{115}\text{In}(n, n')$ ,  ${}^{32}\text{S}(n, p)$ , and  ${}^{27}\text{Al}(n, \alpha)$  reactions, respectively. The solid curves are for the modified Cranberg while the dotted curves are for the Maxwellian form. The suffices I, S, and A in  $\bar{\sigma}$  denote indium, sulphur and aluminum, respectively. In general, the  $\bar{\sigma}$  values are

sensitive to the spectral deformation that is usually indicated by a variation of the  $\bar{E}$ -values, and a variation of the  $\bar{\sigma}$  values for the detectors having the threshold at high energy are large compared to those of the detectors whose threshold energies are comparatively low. This tendency is also clearly noted in the last row of Table 1. The ratio of the  $\bar{\sigma}_I$  values for thermal-to-20 MeV fission is 1.12 and 1.14 for the respective modified Cranberg and Maxwellian forms. This ratio may be further decreased in actual circumstances of criticality accidents. Bondarenko et al.<sup>19)</sup> report that the  $\bar{E}$ -value of fission neutrons induced by fission neutron itself was observed to be 2.013 MeV, leading to 1.067 of the  $\bar{\sigma}$  values for the modified Cranberg and Maxwellian forms, respectively. This phenomenon does strongly hint that indium can yield neutron fluence

values being effectively independent of virgin spectrum in criticality accidents where fission neutrons are completely free from contamination of scattered neutrons. The similar results have been already reported by Yook and Ro.<sup>20)</sup>

On the other hand, threshold detectors with high threshold energy are likely useful in determining the spectral deformations because of their high sensitivity to fissioning types.

As is shown in Figs.1-3, the modified Cranberg form gives the  $\bar{\sigma}$  values higher than the Maxwellian form for indium, while for aluminum the former gives the  $\bar{\sigma}$  values lower than the latter. Obviously this suggests that the Maxwellian form is shifted towards high energy compared with the modified Cranberg form. and subsequently gives the  $\bar{\sigma}$  values higher than the latter for threshold detector whose threshold energy is relatively high. The interesting result is that the  $\bar{\sigma}$  values for the  $^{32}\text{S}(n,p)$  reaction are independent of spectral functions, namely the modified Cranberg and Maxwellian forms. This tendency is also demonstrated in Table 2. In this Table subscripts *C* and *M* in  $\bar{\sigma}$  represent the modified Cranberg and Maxwellian forms, respectively.

Figs.4-6 show a variation of  $\bar{\sigma}$  values as a function of spectral index. On the curves are indicated the upper and lowest limits of  $\bar{E}$ -values. This relation will serve to improve the accuracy in measuring the neutron fluence.

The fluence-to-dose conversion factors as a function of average energy are shown in Fig. 7. The solid lines are those for dose based on kerma while the dotted lines are for maximum doses. As might be expected,

the conversion factor based on the maximum dose is 1.28 times higher than that on kerma. The modified Cranberg form gives slightly  $\bar{d}$  value lower than that of Maxwellian form. The dose conversion factor is relatively insensitive to a variation of spectral functions and of fissioning types. This is also summarized in Table 3. In relation to the result that  $\bar{\sigma}$  values for the  $^{115}\text{In}(n,n')$  reaction is insensitive to fissioning types, this fact makes indium applicable as an integral fast neutron dosimeter in criticality accidents.

In Fig.8 shown are kerma and maximum dose conversion factors for the modified Cranberg form as a function of spectral index which is equal to  $\bar{\sigma}_I/\bar{\sigma}_S$ . These factors, relating to Maxwellian form, are shown in Fig.9. Generally the conversion factors decrease linearly with increasing the spectral index and  $\bar{E}$ -values.

## 6. Conclusions

A neutron dosimetric technique was suggested using activation and threshold detectors in criticality accidents. Dosimetric parameters, that is, the average cross-sections of some threshold detectors and neutron fluence-to-dose conversion factors were then calculated by means of an electronic computer. As a conclusion, the followings can be drawn up:

1) The  $\bar{\sigma}$  values are sensitive to spectral deformation, but their variations of detectors with low threshold energy are small compared to those of detectors whose threshold energies are comparatively high,

2) The  $\bar{\sigma}$  values for the  $^{32}\text{S}(n,p)^{32}\text{P}$  reaction are independent of spectral functions, namely, the modified Cranberg and Maxwellian forms,



3) Maxwellian form is shifted towards high energy in comparison with the modified Cranberg form, and subsequently gives the  $\bar{\sigma}$  values higher than the latter for detectors of which threshold energies are relatively high, and

4) Fluence-to-dose conversion factors are insensitive to both spectral functions and fissioning types.

### Acknowledgments

The authors are grateful to Dr. Kyung Hoon Jung of KAERI for his constant interest and encouragement throughout this work.

### References

1. G. S. Hurst, J. A. Harter, P. N. Hensley, W. A. Mills, M. Slater, and P. W. Reinhardt, Rev. Sci. Instr. 27(3), 153(1956)
2. J. A. Dennis, AERE-R4365(1964)
3. H. Ing and W. G. Cross, Health Phys. 25, 291(1973)
4. R. Gold, Nucl. Sci. Eng. 20, 493(1964).
5. G. Di Cola and A. Rota, Nucl. Sci. Eng. 23, 344(1965)
6. J. Grundl and A. Usner, Nucl. Sci. Eng. 8, 598(1960)
7. C. H. Westcott, J. Nucl. Energy 2, 59(1955)
8. J. Terrell, Phys. Rev. 113(2), 527(1959)
9. S. G. Ro and J. S. Jun, J. Korean Nucl. Soc. 7(2), 119(1975)
10. H. O. Menlove, K. L. Coop, and H. A. Grench, Phys. Rev. 163(4), 1308(1967)
11. H. C. Martin, B. C. Diven, and R. F. Taschek, Phys. Rev. 93(1), 199(1954)
12. E. D. Klema and A. O. Hansen, Phys. Rev.

- 73, 106(1948)
13. P. F. Rago and N. Goldstein, Health Phys. 14, 595(1963)
14. H. Liskien and A. Paulsen, EUR119.e(1963)
15. J. P. Butler and D. C. Santry, Canadian J. Phys., 41 372(1963)
16. W. G. Davey, Nucl. Sci. Eng. 44, 345(1971)
17. ICRU Report-13, (1969)
18. USNBS Handbook-63, (1957)
19. I. I. Bondarenko, B. D. Huzminov, L. S. Kutsayeva, L. I. Prokhorova, and G. N. Smirenkin, Proc. 2nd U.N. Int. Conf. Peaceful Uses of Atomic Energy 1, p. 353, Geneva(1958)
20. C. C. Yook and S. G. Ro, J. Radioisotopes (Japan), 25, April, (1976)

### 一抄 錄一

核臨界事故時에 있어서 速中性子線量의 解析

魯聖基·陸鍾澈\*

韓國原子力研究所

\* 漢陽大學校 工科大学 原子力工學科

### 概 要

核臨界事故時에 放出되는 速中性子가 散亂中性子로 重疊되어 있는 狀態에서 放射化 및 發端放射化檢出器를 利用하여 速中子線量을 測定 및 解析할 수 있는 한 方法을 提案하였으며 이 測定에 있어서 主要因子, 即 몇개의 發端放射化檢出器에 對한 平均核反應斷面積과 中性子當 線量換算係數를 電子計算機로 計算하였다.

그 結果 核分裂中子線의 스펙트럼 測定에는 發端에너지가 높은 檢出器가 有利한 것에 反해 發端에너지가 낮은 것은 散亂媒質이 없는 核臨界裝置의 事故時에 있어서 速中子線의 時積分線束密度 測定計로서 有用한것 같았다. 그리고 硫黃의 (n, p) 核反應에 對한 平均斷面積은 核分裂 中子線의 解析의 表現式에 無關한 것 처럼 보였다.

그밖에 中性子當 線量換算係數의 變化는 核分裂 中子線 스펙트럼의 解析의 表現式과 核分裂形態에 따라 敏感하게 變化되지 않은것 같았다.